

## **Optimum Global Failure Prediction Model of Inconel 600 Thin Plate with Two Parallel Through-Wall Cracks**

**Seong In Moon and Young Jin Kim**

Sungkyunkwan University  
300 Chunchun, Jangan, Suwon 440-746, Korea

**Jin Ho Lee, Myung Ho Song, and Young Hwan Choi**

Korea Institute of Nuclear Safety  
19 Guseong-dong, Yuseong-gu, Daejeon 305-338, Korea  
yjkim50@skku.edu

(Received June 11, 2003)

### **Abstract**

The 40% of wall criterion, which is generally used for the plugging of steam generator tubes, is applied only to a single crack. In a previous study, a total number of 9 failure models were proposed to estimate the local failure of the ligament between cracks, and the optimum coalescence model of multiple collinear cracks was determined among these models. It is, however known that parallel axial cracks are more frequently detected than collinear axial cracks during an in-service inspection. The objective of this study is to determine the plastic collapse model that can be applied to steam generator tubes containing two parallel axial through-wall cracks. Three previously proposed local failure models were selected as the candidates. Subsequently, the interaction effects between two adjacent cracks were evaluated to screen them. Plastic collapse tests for the plate with two parallel through-wall cracks and finite element analyses were performed to determine the optimum plastic collapse model. By comparing the test results with the prediction results obtained from the candidate models, a COD base model was selected as an optimum model.

**Key Words** : coalescence criterion, interaction effect, steam generator tube, plastic collapse, plugging, multiple cracks

### **1. Introduction**

It is commonly requested that steam generator tubes with defects exceeding 40% of wall thickness in depth be should plugged [1~3]. However, this

criterion is known too conservative for some locations and for some types of defects. Many defects detected during in-service inspection show that the formation of multiple cracks at the top of tube sheets is typical; however, there is no reliable

plugging criterion for the tubes with multiple cracks [4~10]. There have been studies on multiple cracks but most of them are limited to elastic analyses and only few studies have been done on steam generator tubes that fail by of plastic collapse [11, 12].

In a previous study, authors performed plastic collapse tests using Inconel 600 plate specimens with two collinear through-wall cracks. The coalescence load of these multiple cracks was also estimated with each of 9 failure models introduced in our previous study. By comparing the estimated results with the test results, the plastic-zone contact model and the reaction force model were selected as two optimum local failure models for the integrity evaluation of steam generator tubes [13]. Unlike two collinear through-wall cracks that behave as one main crack after coalescing with each other, the thin plate or tube with two parallel through-wall cracks is collapsed plastically, following tearing at a crack tip, without any coalescence of the two adjacent cracks. Therefore, a criterion different from that of two collinear through-wall cracks shall be applied to a case of parallel through-wall cracks. A model based on COD (Crack Opening Displacement) was proposed for this application by the authors but the their accuracy was not been evaluated [14].

The objective of this study is to determine the optimum plastic collapse model that can be used to estimate the failure of a steam generator tube containing two parallel axial through-wall cracks. As a first step for this, plastic collapse tests are performed using plate specimens with two parallel through-wall cracks. Their plastic collapse loads are also predicted with three local failure models proposed from our previous studies and the optimum failure model is determined by comparing the estimated results with test results. The second step of this study, which will be covered in another paper, is to apply the

developed optimum failure model to steam generator tubes with multiple parallel axial through-wall cracks.

## **2. Deformation Behavior of Multiple Cracks**

Until now, several criteria have been used to determine the onset of coalescence between two adjacent surface cracks: ASME Sec. XI IWA-3000, BSI PD6493, the contact of surface points, etc. It is known that the criterion based on the contact of surface points shows a good agreement with the experimental results [15~17]. This means that two adjacent cracks coalesce when there is no remaining ligament between them, i.e., the ligament between the cracks can no longer sustain the applied load. Nonetheless, these criteria were developed for applications to pressure vessels and piping whose failure behavior is quite different from that of steam generator tubes. It is necessary to develop a new criterion applicable to the case of large scale yielding because the failure of the cracked steam generator tubes is dominated by large scale yielding.

In our previous studies, the following local and global failure prediction models were proposed to estimate the local or global failure behavior of steam generator tubes.

### **2.1. Two Collinear Through-Wall Cracks**

For the estimation of the local failure of thin plates or tubes with two collinear through-wall cracks, a total of 9 coalescence models were introduced as follows:

(1) Flow Stress Model I (FSM-I) [9, 18~19]: It is assumed that coalescence occurs when the ligament between cracks is fully yielded. A given material is assumed to show elastic-perfectly plastic behavior and yielded at the

flow stress level, which is defined as the mean value between the yield strength and the ultimate tensile strength.

- (2) Flow Stress Model II (FSM-II): The same definition with FSM-I is used but the flow stress is defined as the ultimate tensile strength of a given material.
- (3) Necking Base Model (NBM) [20]: It is assumed that coalescence occurs when the average ligament thickness between cracks begins to decrease rapidly. The true stress-true strain curve is used in this model.
- (4) Stress Base Model I (SBM-I) [21]: It is assumed that coalescence occurs when the average effective stress in the ligament equals the ultimate tensile strength. The true stress-true strain curve is used in this model.
- (5) Stress Base Model II (SBM-II): The same definition with SBM-I is used but the engineering stress-engineering strain curve is used in this model.
- (6) Reaction Force Model (RFM) [22]: It is assumed that coalescence occurs when the reaction force in the ligament between cracks begins to decrease following the increase of the applied load. The true stress-true strain curve is used in this model.
- (7) Plastic Zone Contact Model I (PZC-I): It is assumed that coalescence occurs when plastic zones developed from the crack tips come into contact. This model is based on the contour plot of the effective stress, which comes to the yield strength. The true stress-true strain curve is used in this model.
- (8) Plastic Zone Contact Model II (PZC-II): The same definition with PZC-I is used but this model is based on the contour plot of the effective stress, which comes to the ultimate tensile strength.
- (9) Plastic Zone Contact Model III (PZC-III): The same definition with PZC-I is used but this

model is based on the contour plot of the effective stress, which comes to the true stress value of the ultimate tensile strength.

The above local failure models were used to estimate the coalescence loads of two collinear through-wall cracks existing in thin plates or tubes. By comparing the predicted results with the test results, the Reaction Force Model and Plastic Zone Contact Model II & III were selected as the optimum local failure models for the coalescence evaluation of multiple collinear cracks existing in thin plates or steam generator tubes.

## 2.2. Two Parallel Through-Wall Cracks

Unlike the collinear through-wall cracks, the thin plate or tube with two parallel through-wall cracks is collapsed plastically without any coalescence of two adjacent cracks. Thus, the failure prediction model applicable to this case was proposed in our previous study as follows [14]:

- COD Base Model (CBM): It is assumed that the failure of the thin plate or tube with two parallel through-wall cracks occurs when the COD at each of two parallel cracks is equal to the COD at the failure pressure of a single crack.

## 3. Plastic Collapse Tests of Thin Plates with Two Parallel Through-Wall Cracks

To determine the plastic collapse loads of thin plate specimens with two parallel through-wall cracks, a series of plastic collapse tests was carried out.

### 3.1. Material and Specimen

Test specimens were made of Inconel 600 plate material. The thickness of the plate is 6 mm and the chemical composition and tensile properties of the material are given in Tables 1 and 2,

**Table 1. Chemical Composition of Inconel 600 Plate**

Element	C	Mn	Si	P	S	Ni	Cr
Wt. %	404*	0.22	0.37	N.D.	N.D.	74.4	15.7
Element	Co	Ti	Al	Cu	Fe	N	
Wt. %	0.056	0.16	0.26	0.09	9.7	69.6*	

\*Unit: ppm

**Table 2. Mechanical Properties of Inconel 600 Plate**

Yield strength (MPa)	Tensile strength (MPa)	Young's modulus (GPa)	Elongation (%)	Poisson's ratio
329	662	213	44	0.3

**Fig. 1. Geometry and Size of Test Specimen**

respectively. Fig. 1 shows the geometry of the specimen. Specimens were fabricated in T-L direction and notches were wrought by using the Electro-Discharge Machining (EDM) method. Plastic collapse tests were carried out for plates containing two parallel through-wall cracks where the crack lengths,  $2c$ , are 5, 8, and 13 mm and the distance between the cracks,  $d$ , is are 1, 2, and 4 mm, respectively. Additional tests were also performed for the plates with a single crack of  $2c = 5, 8$ , and 13 mm, respectively.

### 3.2. Test Facilities and Method

Plastic collapse tests were performed by displacement control and a universal testing

**Fig. 2. Test Facilities**

machine with a 25-ton capacity (Instron model 8802) was used. Both ends of the specimen were fixed using hydraulic grips, as shown in the test facilities of Fig. 2. When the applied load increases, the process of crack coalescence was observed using a high resolution camera, with a magnifying power of 100. The Strain gauge, the COD gauge, and the extensometer signals were continuously stored in a notebook PC, via an A/D converter.

### 3.3. Test Results

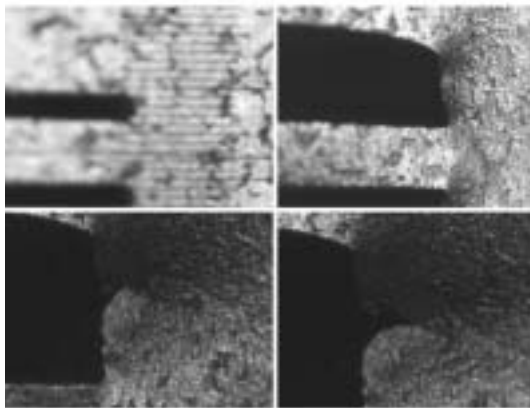
The failure behavior of the specimen with two parallel cracks is monitored using a high resolution camera, and typical failure behavior is shown in Fig. 3. As the load increases, crack tips are blunted and tearing occurs at the crack tip first.

**Table 3. Failure Loads of Single-cracked Plates**

Crack size (mm)	Failure load (kN)
$2c=5$	47.2
$2c=8$	42.3
$2c=13$	37.7

**Table 4. Failure Loads of Double-cracked Plates**

Crack size (mm)	Failure load (kN)
2c=5, d=1	52.9
2c=5, d=2	52.4
2c=5, d=4	50.9
2c=8, d=1	47.4
2c=8, d=2	47.3
2c=8, d=4	47.7
2c=13, d=1	41.5
2c=13, d=2	42.3
2c=13, d=4	42.5

**Fig. 3. Process of Plastic Collapse**

Then, the crack growth is dominated by the crack torn first, the outside ligament collapses plastically, and finally the specimen is broken into two parts. Tables 3 and 4 indicate the plastic collapse loads of single-cracked plates and double-cracked plates, respectively.

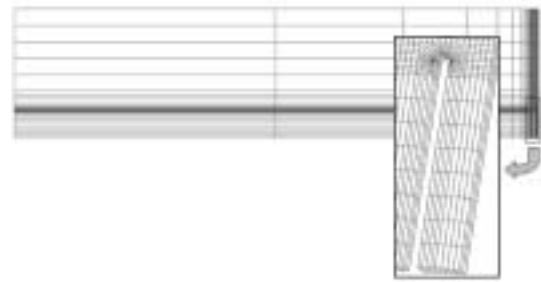
#### 4. Failure Prediction Model of Thin Plates with Two Parallel Cracks

For the determination of the optimum failure prediction model of thin plates with two parallel through-wall cracks, the local and global failure models mentioned above are reevaluated, and

their results are compared with the experimental results. By considering the deformation characteristics of the two parallel through-wall cracks, just 3 models including the PZC-II, PZC-III, and CBM model were selected for this purpose.

#### 4.1. Finite Element Analysis

The deformation behavior of two parallel through-wall cracks was estimated by performing three-dimensional elastic-plastic finite element analyses. ABAQUS Version 5.8 package was used

**Fig. 4. Finite Element Mesh of Plate with Two Parallel Cracks****Table 5. Estimated Failure Loads of Plates with Two Parallel Through-wall Cracks**

2c & d (mm)	Failure load (kN)			
	PZC-II	PZC-III	CBM	Exp. Results
2c=5, d=1	36.4	43.9	50.9	52.9
2c=5, d=2	39.6	50.5	50.5	52.4
2c=5, d=4	44.4	54.3	49.7	50.9
2c=8, d=1	32.9	39.7	47.3	47.4
2c=8, d=2	36.4	45.6	47.1	47.3
2c=8, d=4	40.5	50.2	46.4	47.7
2c=13, d=1	30.3	34.4	42.6	41.5
2c=13, d=2	32.6	39.8	42.8	42.3
2c=13, d=4	36.3	44.3	42.5	42.5

in this analysis. Fig. 4 shows the finite element mesh of the test specimen. An eighth of the specimen was modeled using the symmetry. The finite element mesh consists of 20-node quadratic brick elements with reduced integration points. The notch tip was rounded to the same radius of curvature as the specimen,  $\rho = 0.15$  mm. Finite element analyses were carried out for the cases where the crack length,  $2c$ , are 5, 8, and 13 mm and the distances between the two adjacent crack,  $d$ , are 1, 2, and 4 mm, respectively. The plastic collapse loads of thin plates were estimated by using each of three failure prediction models. The analysis results are summarized in Table 5.

## 5. Results and Discussion

### 5.1. Accuracy of Failure Prediction Models

The failure loads obtained from the plastic collapse tests for single-cracked plates and double-

cracked plates were summarized in Tables 3 and 4. The failure load of the thin plate decreases as the crack length increases but the effects of the distance between two cracks are negligible. It is, however, noted that the failure load of the plate with two parallel through-wall cracks is higher than that with a single through-wall crack.

Table 5 shows the comparison results between the estimated and the experimental data. As  $2c$  is 8 mm,  $d$  is 2 mm, and the applied load increases, the changes of plastic zone size along the mid-plane between either surfaces of the specimen are shown in Fig. 5. Since the growth of the plastic zone in the mid-plane of the specimen is slower than that on the surface of the specimen, the mid-plane of the plate was chosen as a reference plane for the failure prediction in the PZC model. The estimation results derived from the PZC-II model showed a large discrepancy with the experimental results. In the comparison of the estimated results with the experimental results, the estimated failure

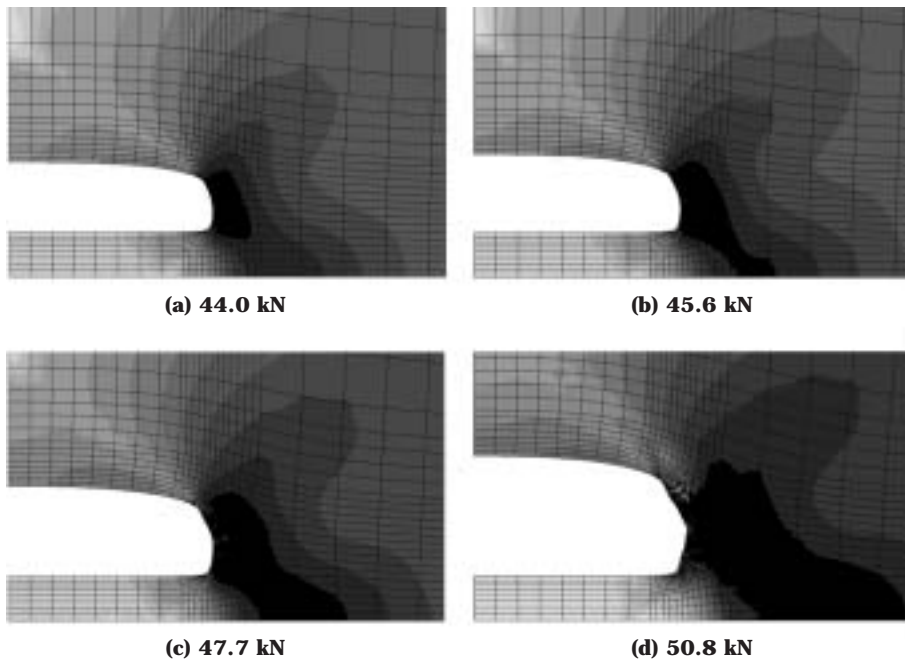


**Fig. 5. Changes of Plastic Zone Size Along the Mid-plane**

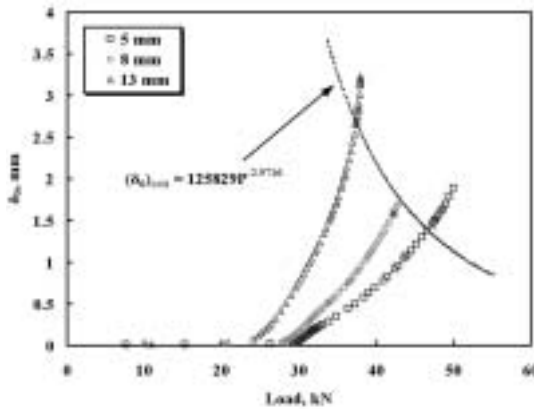


**Fig. 6. Critical COD Data at the Center of a Single Crack**

loads obtained using the PZC-III model indicated the maximum difference of 17% and the average difference of 5.3%.

The COD changes at the crack center,  $\delta_0$ , were calculated by finite element analyses. Fig. 6 shows the changes of  $\delta_0$  to the applied load when a single crack exists in the plate. In Fig. 6, the failure loads of the plates were measured by experiment and the corresponding values of  $\delta_0$  were marked with the symbol 'x'. These values are defined as a critical value of  $\delta_0$  in this paper and denoted as  $(\delta_0)_{crit}$ . From the  $(\delta_0)_{crit}$  values, the following regression line was derived.

$$(\delta_0)_{crit} = 125829P^{-3.0188} \quad (1)$$

where  $P$  is the applied load. The above power law expression was obtained using the least square fit and illustrated as a dotted line in Fig. 6. This curve was used to determine the critical COD values at the crack center and the associated failure loads of the plates with two parallel through-wall cracks. The changes of  $\delta_0$  values in the plate with a pair of parallel through-wall cracks were obtained from finite element analyses and plotted in Fig. 7. In the CBM model, the failure loads of the plate with a pair of parallel cracks are determined from the

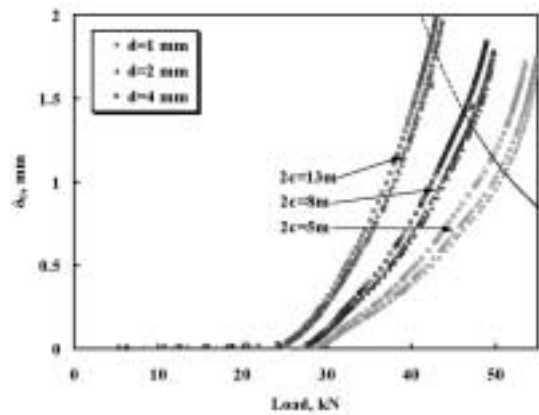


**Fig. 7. Changes of  $\delta_0$  Values (two parallel cracks)**

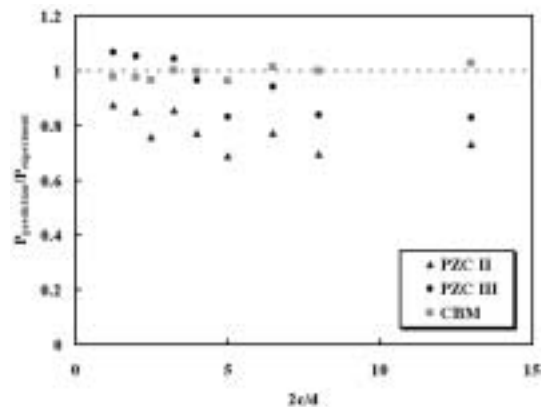


**Fig. 8. Comparison of Estimated Results with Experimental Results**

intersection point between the  $(\delta_0)_{crit}$  -  $P$  curve of Eq. (1) and the  $\delta_0$  -  $P$  curve of the two parallel cracks. The failure loads estimated by applying the CBM model showed a good agreement with the experimental results. The maximum and the average difference are 3.7% and 1%, respectively.

In Fig. 8, all the estimated results are compared with the experimental results. The estimation accuracy of the failure models is in the following order, from highest to lowest: (1) CBM, (2) PZC-III, and (3) PZC-II model. The accuracy of the CBM model is excellent; however only 3 experimental data were used to obtain the regression line of Eq. (1), which affects the



accuracy of the estimation results greatly.

For more reliable estimation using the CBM model, a limit load solution is adopted that is widely used to estimate the plastic collapse load of the plate containing a single crack [23].

$$P_L = \sigma_f \cdot 2(W - c) \cdot t \quad (2)$$

where  $W$  is a half of the specimen width and  $t$  is the thickness of the specimen. The flow stress,  $\sigma_f$ , is defined as follows:

$$\sigma_f = k(\sigma_Y + \sigma_U) \quad (3)$$

where  $k$  is the flow stress factor and  $\sigma_Y$  and  $\sigma_U$  are the yield and ultimate tensile strength, respectively. Since the geometry and tensile properties of the plate specimen are given, the only unknown variable in Eq. (2) and (3) is the flow stress factor  $k$ . The  $k$  values are calculated from Eq. (2) and (3) and the measured plastic collapse loads of Table 3 are 0.51, 0.51 and 0.54 for the cases of  $2c = 5$ , 8, and 13 mm, respectively. In this paper,  $k = 0.51$  was used to obtain the plastic collapse loads of the single-cracked plates.

Fig. 9 shows the values of  $(\delta_0)_{crit}$  obtained using Eq. (2) instead of the experimental data. The  $(\delta_0)_{crit}$

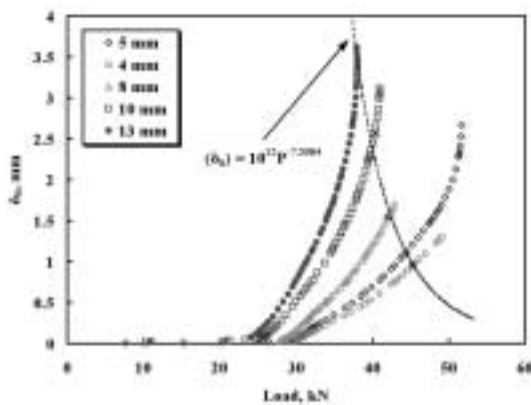


**Fig. 9. Critical COD Data at the Center of a Single Experimental Results Crack (FEM)**

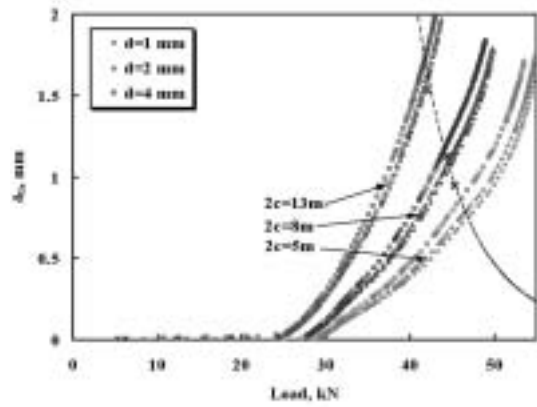


**Fig. 10. Changes of  $\delta_0$  Values**

-  $P$  curve was derived using the form of a power law and the least square method:

$$\sigma_f = k(\sigma_Y + \sigma_U) \quad (4)$$

The changes of  $\delta_0$  values with load and the obtained regression line are plotted in Fig. 10. As before the failure loads of the plate with a pair of parallel cracks are determined from the intersection point between the  $(\delta_0)_{crit} - P$  curve of Eq. (4) and the  $\delta_0 - P$  curve of the two parallel cracks. This approach using Eq. (2) instead of the experimental data is defined as the COD Base

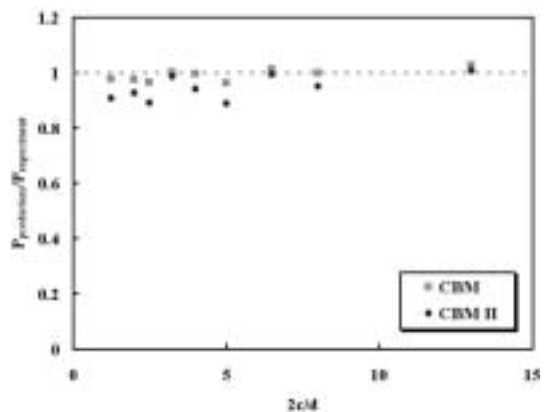


**Fig. 11. Comparison of Estimated Results with (two parallel cracks) Experimental Results (CBM & CBM-II model)**



Model II (CBM-II) in this paper. Both results obtained from the CBM and CBM-II model are plotted in Fig. 11. In the comparison with the experimental results, the maximum and the average difference of the CBM-II model are 11.1% and 5.7%, respectively. The accuracy of the CBM-II model is slightly lower than that of the CBM model.

### 5.2. Interaction Effects Between Two Parallel Cracks

The experimental results show that the plate with a pair of parallel through-wall cracks has higher plastic collapse load than the plate with a single through-wall crack. Three-dimensional elastic and elastic-plastic finite element analyses were performed to investigate the root cause of this. Both elastic analysis, based on the stress intensity factor  $K$ , and elastic-plastic analysis, based on the  $J$ -integral, were carried out. The following two factors were defined to explain the degree of interaction in the elastic analysis and the elastic-plastic analysis, respectively.

$$K_{ratio} = \frac{K_D}{K_S} \quad (5)$$

$$K_{ratio} = \frac{K_D}{K_S} \quad (6)$$

where the subscript 'S' and 'D' denote a single crack and two parallel cracks, respectively.

Table 6 shows the values of  $K_{ratio}$  when  $2c = 8$  mm

**Table 6. Evaluation of Interaction Effects Based on K**

Crack size(mm)	KS (MPa · m)	KD (MPa · m)	Kratio
2c=8, d=1		176	0.721
2c=8, d=2	245	182	0.742
2c=8, d=4		191	0.790

**Table 7. Evaluation of Interaction Effects Based on J**

Crack size (mm)	P (MPa)	JS (MPa · m)	JD (MPa · m)	Jratio
2c=8, d=1	27.8	12.0	6.4	0.553
	28.3	18.4	10.2	0.554
	30.1	60.8	34.7	0.571
2c=8, d=2	27.8	12.0	6.7	0.558
	28.5	23.1	14.5	0.628
	30.1	60.8	39.2	0.645
2c=8, d=4	28.1	15.2	11.1	0.730
	28.9	32.4	22.7	0.701
	30.3	67.3	47.8	0.710

and  $d = 1, 2$ , and  $4$  mm, respectively. It is shown in Table 6 that  $K_{ratio}$  decreases as  $d$  decreases. This beneficial interaction effect ( $K_{ratio} < 1$ ) becomes enlarged as the distance becomes smaller. Table 7 shows the values of  $J_{ratio}$  when  $2c = 8$  mm and  $d = 1, 2$ , and  $4$  mm, respectively. Like  $K_{ratio}$ ,  $J_{ratio}$  also decreases as  $d$  decreases. Higher negative interaction effects are observed for a shorter distance and  $J_{ratio}$  shows greater negative interaction effects than  $K_{ratio}$  in all cases. It is thought that the beneficial interaction effects occur because the stress fields in the plate with two parallel cracks change less rapidly around the crack tips than those in the plate with a single crack, or in the plate with two collinear cracks. Accordingly, stress relaxation takes place near the crack tips and the failure load of the plate with two parallel cracks becomes higher than that of the plate with a single crack, or of the plate with two collinear cracks.

### 5.3. Optimum Failure Prediction Model

In this study, 3 failure prediction models were introduced to estimate the plastic collapse loads of thin plates with two parallel through-wall cracks,

and their estimation results were compared with the experimental results. The model with the highest accuracy of prediction was found to be the CBM (including the CBM-II) model, followed by the PZC-III model, and finally the PZC-II model. The prediction results of the PZC-II model were quite poor. As judged from the experimental results and from the finite element analysis results on the interaction effects, the negative interaction effects are expected to be weakened with the increase of the distance between cracks. However, the results of the PZC-III model are directly opposite to these results. The results of the CBM model (including the CBM-II model) show a good agreement with the experimental results and explain the negative interaction effects well. From the above results, the CBM model was selected as the optimum failure prediction model for the plate with two parallel through-wall cracks.

## 6. Conclusions

In this study, plastic collapse tests using Inconel 600 plate specimens with two parallel through-wall cracks were performed. Three failure prediction models were proposed to estimate the plastic collapse loads of thin plates containing two parallel through-wall cracks, and their estimation results were compared with the experimental results.

From the experimental results and the finite element analysis results on the interaction effects, it was confirmed that the plates with two parallel through-wall cracks have higher plastic collapse loads than those plates with a single through-wall crack. Stress relaxation takes place around the crack tips; therefore, the failure load of the plate with a pair of parallel cracks becomes higher than that of the plate with a single crack.

Among three failure prediction models, the CBM model predicted the failure loads of the thin

plates containing two parallel through-wall cracks quite accurately. In addition, it explains the negative interaction effects well. Thus, the CBM model was selected as the optimum failure prediction model for the plate with two parallel through-wall cracks. The second step of this study will involve applying the obtained optimum failure prediction model to the steam generator tubes with two parallel through-wall cracks for the estimation of failure loads.

## References

1. USNRC, "NUREG/CR-6365, Steam Generator Tube Failures "(1996).
2. USNRC Regulatory guide 1.121, "Bases for Plugging Degraded PWR Steam Generator Tubes "(1976 ).
3. ASME, " Rules for Construction of Nuclear Power Plant Components, " ASME Bolier and Pressure Vessel Code, Sec. III (1998).
4. Cochet, B. and Flesch, B., " Crack Stability Criteria in Steam Generator Tubes, " 9th Int. Conference on SMiRT, Vol. D, pp.413-419 (1987).
5. Yu, Y.J., Kim, J.H., Kim, Y., and Kim, Y.J., " Development of Steam Generator Tube Plugging Criteria for Axial Crack, " *ASME PVP*, Vol. 280, pp.79-83 (1994).
6. Kim, H.D., Chung, H.S., and Hong, S.R., " Discussion on Operation Leakage Criteria of Ulchin Unit 1&2 Steam Generators, " *Proceedings of the Korean Nuclear Society Autumn Meeting* (1999).
7. Kim, H.D, Kim, K.T., and Chung, H.S., " Structural integrity assessment on axial PWSCC of steam generator tubes, " *Proceedings of the Korean Nuclear Society Autumn Meeting* (1999).
8. Gorman, J. A., Harris, J. E., and Lowenstein, D.B., " Steam Generator Tube Fitness-for-

- Service Guidelines, " AECB Report No. 2.228.2, pp. 220 (1995).
9. Lee, J.H., Park, Y.W., Song, M.H., Kim, Y.J., and Moon, S.I., " Determination of Equivalent Single Crack based on Coalescence Criterion of Collinear Axial Cracks, " *Nuclear Engineering and Design*, Vol.205, pp. 1-11 (2000).
  10. Kim, J.S. et al., " Investigation Report for Steam Generator Tubes Pulled out from Ulchin #1, " October (1999).
  11. Y. Murakami, 1987, " Stress Intensity Factors Handbook, " pp.204-205.
  12. Cho, Y.J., " A Study on the Interaction Effect of Adjacent Semi-Elliptical Crack, " Master's Thesis (1990).
  13. Moon, S.I., Kim, Y.J., Kim, Y.J., Park, Y.W., Song, M.H., and Lee, J.H., " Determination of Optimum Local Failure Model of a Steam Generator Tube with Multiple Through-wall Cracks, " Proceedings of the Korean Society of Mechanical Engineers - Part of Material and Fracture Spring Meeting, pp.87~93 (2002).
  14. Park, Y.W., Song, M.H., Lee, J.H., Moon, S.I., and Kim, Y.J., " Investigation on the Interaction Effect of Two Parallel Axial Through-Wall Cracks existing in Steam Generator Tube, " *Nuclear Engineering and Design*, Vol.214, pp. 13-23 (2002).
  15. Kim, Y. J., Choy, Y. S., and Lee, J. H., " Development of Fatigue Life Prediction Program for Multiple Surface Cracks, " ASTM STP 1189, pp.536-550 (1993).
  16. Shibata, K., Yokoyama, N., Ohba, T., Kawamura, T., and Miyazono, S., " Growth Evaluation of Fatigue Cracks from Multiple Surface Flaws (I), " *J. Japanese Nuclear Society*, Vol. 28, No. 3, pp.250-262 (1985).
  17. Shibata, K., Yokoyama, N., Ohba, T., Kawamura, T., and Miyazono, S., " Growth Evaluation of Fatigue Cracks from Multiple Surface Flaws (II), " *J. Japanese Nuclear Society*, Vol. 28, No. 3, pp.258-265 (1986).
  18. Park, Y. W., Song, M. H., and Lee, J. H., " Steam Generator Tube Integrity Program, " KINS/RR-001 (2000).
  19. Lee, J.H., Park, Y.W., Song, M.H., Kim, Y.J., and Moon, S.I., " Evaluation of Plugging Criteria an Steam Generator Tubes and Coalescence Model of Collinear Axial Through-Wall Cracks, " *J. Korean Nuclear Society* Vol. 32, pp.465-476 (2000).
  20. Diercks, D. R., " Steam Generator Tube Integrity Program Monthly Report, " ANL, August (2000).
  21. Diercks, D. R., " Steam Generator Tube Integrity Program Monthly Report, " ANL, September (2000).
  22. S. B. Lumbert, W. J. Alcott, A. G. Glover, " Numerical Simulation of Interaction Effects for Through Cracks in Plastic Collapse, " Unpublished Paper.
  23. Miller, A.G., " Review of Limit Loads of Structures Containing Defects, " *Int. J. Pres. & Piping* Vol. 32, pp.197~327 (1988).